

Signature of a light charged Higgs boson from top quark pairs at the LHC

YaLu Hu^{1,2}, ChunHao Fu^{1,2} and Jun Gao^{1,2}

¹*NPAC, Shanghai Key Laboratory for Particle Physics and Cosmology & School of Physics and Astronomy, Shanghai Jiao Tong University, Shanghai 200240, China*

²*Key Laboratory for Particle Astrophysics and Cosmology (MOE), Shanghai 200240, China*



(Received 17 June 2022; accepted 26 September 2022; published 11 October 2022)

The charged Higgs boson is a smoking gun of extensions of the standard model with multiple Higgs doublets, and has been searched for at various collider experiments. In this paper, we study the signature of a light charged Higgs boson produced by top quark pairs at the Large Hadron Collider (LHC), with subsequent three-body decays into a W boson and a pair of bottom quarks. Cross sections on final states of two W bosons plus four bottom quarks have been measured by the ATLAS Collaboration at the LHC 13 TeV. We reinterpret the experimental data under the scenario of a light charged Higgs boson and find improved agreements. We obtain the first limit from LHC direct searches on the total branching ratio of the three-body decay, $\text{Br}(t \rightarrow H^+ b) \times \text{Br}(H^+ \rightarrow W^+ b \bar{b})$, and the strongest direct constraints on the parameter space of a class of type-I two-Higgs-doublet models.

DOI: [10.1103/PhysRevD.106.L071701](https://doi.org/10.1103/PhysRevD.106.L071701)

I. INTRODUCTION

The successful operation of the CERN Large Hadron Collider (LHC) and the ATLAS and CMS experiments has led to the discovery of the Higgs boson, the final piece of the standard model (SM) [1,2] of particle physics. Ten years after the discovery it remains mysterious: how the masses of fermions are arranged in a pattern of hierarchy, and if the SM Higgs boson is the only elementary particle with spin zero. A natural extension of the SM Higgs sector is to include multiple Higgs doublets, for instance, the well-motivated two-Higgs-doublet models (2HDMs) [3,4]. The charged Higgs boson is a smoking-gun signature of such new physics models and has received a lot of attentions recently. Direct searches on the charged Higgs boson have been carried out previously at LEP [5], Tevatron [6,7], and now at the LHC [8,9]. Constraints on branching ratios of various decay channels of the charged Higgs boson have been obtained, depending on its mass. We expect improved sensitivities at the upcoming run of the LHC with high luminosities, which may lead to a discovery of the charged Higgs boson or even stringent limits.

The searches of a light charged Higgs boson at the LHC, namely, with mass smaller than the difference of the masses

of the top quark and the bottom quark, benefit from the large production cross sections of the top quark pair which decays into the charged Higgs boson and a bottom quark. A light charged Higgs boson can undertake several possible decays [10–13], for instance in the 2HDMs into $\tau^+ \nu_\tau$, $c \bar{s}$, $c \bar{b}$, $t^{(*)} \bar{b}$, and $W^+ A$ if the mass of the CP -odd Higgs boson A is below the threshold. The latter two decays can both lead to $W^+ b \bar{b}$ final states either directly or via the cascade decay of A , which can be dominant over the two-body decays. There exist many theoretical studies demonstrating the potential of the $W^+ b \bar{b}$ decay channel for exploring the parameter space of the 2HDMs [14–20]. However, to our best knowledge, there are no dedicated experimental searches reported so far at the LHC on this three-body decay channel.

In this Letter, we utilize a measurement on inclusive and differential fiducial cross sections of final states with two W bosons and four bottom quarks by the ATLAS Collaboration at the LHC 13 TeV with an integrated luminosity of 36 fb^{-1} [21]. We reinterpret the experimental data under the scenario of a light charged Higgs boson, and find improved agreements with the data. Here one of the top quarks decays into a charged Higgs boson and the other follows the SM decay into a W boson and a bottom quark. We obtain the first limit from LHC direct searches on the total branching fraction of the three-body decay, $\text{Br}(t \rightarrow H^+ b) \times \text{Br}(H^+ \rightarrow W^+ b \bar{b})$, for a charged Higgs boson with mass smaller than the top quark. Our result sets strong constraints on the parameter space of type-I 2HDMs.

Published by the American Physical Society under the terms of the [Creative Commons Attribution 4.0 International license](https://creativecommons.org/licenses/by/4.0/). Further distribution of this work must maintain attribution to the author(s) and the published article's title, journal citation, and DOI. Funded by SCOAP³.

II. THEORY AND DATA COMPARISON

ATLAS measured final states including a pair of W bosons and four bottom quarks and compared with SM predictions from QCD production of a pair of top quarks associated with a pair of bottom quarks with subsequent decays. The measurement has been separated into the pure leptonic channel where one of the W bosons decays into an electron and the other into a muon, and the lepton plus jets channel where one of the W bosons decays into jets and the other into either a muon or electron [21]. We refer to them as leptonic and jet channels for simplicity in the following sections. The W boson can decay to the electron and muon either directly or via an intermediate τ lepton, where the latter contributes about 10% to the cross sections. For each channel the signal region is further classified as that with at least four b jets and that with at least three b jets, since one of the bottom quarks can be out of experimental acceptance. The results on inclusive and differential fiducial cross sections have been unfolded to particle level to ensure comparisons with theoretical predictions from MC event generators. Detailed definitions on the fiducial region can be found in the experimental publication [21] and are also implemented in the public Rivet [22] analysis routine. We note that there is another measurement on similar final states by the CMS Collaboration [23]. However, we conclude that the CMS measurement cannot be used in our study of the charged Higgs boson since it requires reconstructions of the top quarks following the SM decay mode.

Theoretical predictions on the binned cross sections in the presence of a light charged Higgs boson can be expressed as

$$\begin{aligned}\sigma_{\text{pre}}^{\text{bin}} &\equiv \sigma_{\text{SM}}^{\text{bin}} + \sigma_{H^+}^{\text{bin}} \\ &= \sigma_{\text{SM}}(t\bar{t}b\bar{b})\epsilon_{\text{SM}}^{\text{bin}} + 2B_{H^+}^{\text{sig}}\sigma_{\text{SM}}(t\bar{t})\epsilon_{H^+}^{\text{bin}}\end{aligned}\quad (1)$$

assuming the branching ratio of the top quark decays into the charged Higgs boson is small. $\sigma_{\text{SM}}(t\bar{t}b\bar{b})$ is the SM cross section on QCD production of four heavy quarks, and $\epsilon_{\text{SM}}^{\text{bin}}$ represents the efficiency for the prescribed kinematic bin including branching fractions of SM decays of the W boson. There are also other SM processes contributing to the same final states which have been subtracted from the experimental data already. Contributions from the charged Higgs boson have been factorized into the SM cross section on QCD production of the top quark pair, the efficiency, and the total branching fraction $B_{H^+}^{\text{sig}}$ for the full decay chain of $t \rightarrow H^+ b \rightarrow W^+ b\bar{b}$. The factor of 2 in Eq. (1) is due to the fact that the charged Higgs boson arises from decays of both the top quark and antiquark. Nonresonant production cross section of a light charged Higgs boson is generally below 10% of the cross section for on-shell production of the top quark pair with subsequent decays [24]. We do not include the nonresonant contributions for simplicity. We treat $B_{H^+}^{\text{sig}}$ as an input of the signal strength of new physics,

and derive the efficiency $\epsilon_{H^+}^{\text{bin}}$ from MC simulations that only depend on masses of the Higgs bosons.

We generate event samples with MG5_aMC@NLO [25] followed by parton showering (PS) and hadronizations with PYTHIA8 [26] in the four flavor number scheme (4FS), and analyze the events with the public routine of the ATLAS analysis in Rivet [22]. We use CT18 parton distribution functions (PDFs) [27] and a top (bottom) quark pole mass of 172.5 (4.75) GeV in simulations, and set the default renormalization and factorization scales to the sum of transverse energy of all final states divided by two. For MC simulations of the charged Higgs boson, we use a model file of the general 2HDMs generated with FeynRules [28]. The efficiency $\epsilon_{H^+}^{\text{bin}}$ is calculated with event samples generated at leading order in QCD matched with PS. We set the total cross section of SM top quark pair production to 838.5 pb at LHC 13 TeV, calculated with Top++2.0 [29,30] at next-to-next-to-leading order (NNLO) and next-to-next-to-leading logarithmic accuracy in QCD. We include two scenarios on the three-body decay of the charged Higgs boson with a mass between 110 and 160 GeV. In the first case, scenario \mathcal{A} , we assume that the additional neutral Higgs bosons are heavier than H^+ and the three-body decay goes directly as $H^+ \rightarrow t^{(*)}\bar{b} \rightarrow W^+ b\bar{b}$. In scenario \mathcal{B} , we assume a CP -odd Higgs boson A with a mass $M_A = M_{H^+} - 85$ GeV, similar to the one in Ref. [31]. The three-body decay goes through a cascade $H^+ \rightarrow W^+ A(b\bar{b})$.

For the SM predictions, we calculate $\sigma_{\text{SM}}^{\text{bin}}$ directly using event samples of $t\bar{t}b\bar{b}$ generated at next-to-leading order (NLO) in QCD matched with parton showering. We find good agreements of our SM predictions with those predictions shown in the ATLAS analysis [21]. In the remaining part of our study we instead use the theoretical predictions reported in the ATLAS analysis directly since comprehensive estimations of theoretical uncertainties are available. To be specific, for the inclusive fiducial cross sections, we take the theoretical predictions from SHERPA2.2 [32] at NLO + PS in 4FS. The theoretical uncertainties are obtained by varying the renormalization and factorization scales by factors of 0.5 and 2.0 and including PDF uncertainties from NNPDF3.0 NNLO PDFs [33]. For normalized fiducial distributions, we take the predictions from POWHEG+PYTHIA8 in the 4FS for $t\bar{t}b\bar{b}$ production [34], and in the 5 flavor number scheme (5FS) for $t\bar{t}$ production [35], both at the accuracy of NLO + PS. In the 5FS, there are three predictions with different tunes of POWHEG and PYTHIA8 [36], and additional bottom quarks are generated from PS. We take midpoints of the envelope of the four predictions as the central prediction and half width of the envelope as theoretical uncertainties. The PDF uncertainties are negligible for normalized distributions and are thus not included. We have checked that the choice of the nominal theoretical prediction on the SM $t\bar{t}b\bar{b}$ production has little impact on our final results. There are also several recent calculations on the SM predictions at

NLO + PS accuracy [37,38], and at NLO including full nonresonant and off-shell contributions with leptonic decays of the W bosons [39–41].

We perform a survey on the inclusive and various differential fiducial cross sections measured by ATLAS and select three data sets. The first set is on the inclusive fiducial cross sections of the leptonic and jet channel with three and four b jets respectively. The other two are normalized distributions of invariant mass of the pair of two closest b jets in ΔR , $m_{bb}^{\Delta \min}$, for the leptonic and jet channel, respectively. Distributions of $m_{bb}^{\Delta \min}$ are most sensitive to the charged Higgs boson which tends to generate a smaller invariant mass for the two closest b jets. We drop the last bin in each of the two distributions since they are not independent from the rest for normalized distributions. We show comparisons between theory and data on the inclusive fiducial cross sections and the normalized $m_{bb}^{\Delta \min}$ distribution of the leptonic channel in Fig. 1, for the SM and the SM with a charged Higgs boson of scenario \mathcal{B} in addition. We take a mass of 140 GeV of the charged Higgs boson and a signal strength of 0.4% for demonstration. Both theoretical predictions are normalized to the central measurements. The bands and error bars represent the total experimental and theoretical errors,

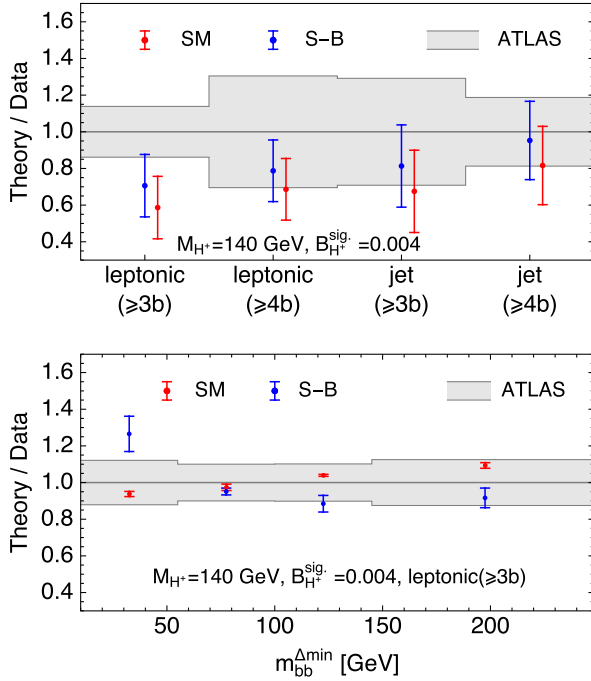


FIG. 1. Comparisons of theory and data on the inclusive fiducial cross sections and the normalized $m_{bb}^{\Delta \min}$ distribution of the leptonic channel, for the SM and the SM with a charged Higgs boson of scenario \mathcal{B} in addition. We take a mass of 140 GeV and a signal strength of 0.4% for demonstration. Theory predictions are normalized to the central measurements. The bands and error bars represent the total experimental and theoretical errors, respectively.

respectively. For the normalized distributions, the theoretical uncertainties increase when including contributions from the charged Higgs boson, due to the uncertainties propagated from the SM inclusive fiducial cross sections. We find the charged Higgs boson brings fiducial cross sections closer to central of the ATLAS data and leads to a significant increase of $m_{bb}^{\Delta \min}$ distribution in the first bin.

The log-likelihood function χ^2 summed over the chosen data sets is calculated as

$$\chi^2(M_{H^+}, B_{H^+}^{\text{sig}}) = \sum_i \frac{(\sigma_{\text{pre}}^{\text{bin},i} - \sigma_{\text{dat}}^{\text{bin},i})^2}{\delta_{\text{sta},i}^2 + \delta_{\text{sys},i}^2 + \delta_{\text{th},i}^2}, \quad (2)$$

where the denominator includes statistical, systematic, and theoretical uncertainties, respectively. $\sigma_{\text{dat}}^{\text{bin},i}$ is the central measurement of the cross section in the i th bin. We cannot include distributions on different kinematic variables at once since they are fully correlated in statistics. We plot χ^2 contours on the plane of the mass of the charged Higgs boson and the signal strength in Fig. 2 for the scenario \mathcal{B} with a total number of experimental data points of 12. The results are similar for the scenario \mathcal{A} which is not shown here. We have subtracted the χ^2 of pure SM predictions in the contours, which is 6.9 units. For both scenarios the best fit is found at M_{H^+} close to 110 GeV and with a total branching fraction $B_{H^+}^{\text{sig}}$ of about 0.3%~0.4%. The χ^2 is lower by about 2 units compared to the SM case. Inclusion of contributions from the charged Higgs boson leads to moderate improvement on description of the data especially because of enhancements to the inclusive fiducial cross sections.

We can deduce upper limits on the total branching fraction of $t \rightarrow H^+ b \rightarrow W^+ b b \bar{b}$ for fixed values of M_{H^+} .

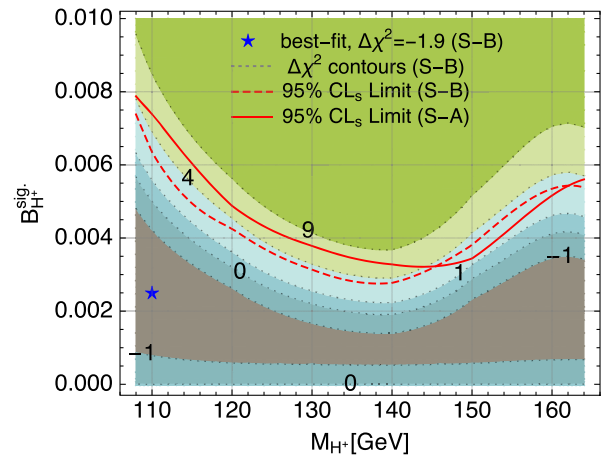


FIG. 2. χ^2 contours on the plane of the mass of the charged Higgs boson and the signal strength for the scenario \mathcal{B} , with χ^2 of the pure SM predictions subtracted. 95% CLs limits on the signal strength for the two scenarios of the charged Higgs boson as functions of the mass are also shown.

We use the CLs method [42] together with the χ^2 function. Note here we only include the two datasets of normalized distributions (8 bins in total) for calculations of the χ^2 . Upper limits on $B_{H^+}^{\text{sig}}$ for a fixed M_{H^+} at a confidence level $1 - \alpha'$ are determined as

$$\hat{\mu} + \Delta_\mu \Phi^{-1}(1 - \alpha' \Phi(\hat{\mu}/\Delta_\mu)), \quad (3)$$

where $\hat{\mu}$ is the best fit of $B_{H^+}^{\text{sig}}$ with fixed M_{H^+} , and Δ_μ is the uncertainty estimated by requiring $\Delta\chi^2 = 1$ compared to the best fit. Φ is the cumulative distribution function of normal distribution. We plot the 95% CLs limits for the two scenarios of the charged Higgs boson as functions of the mass in Fig. 2. The best limit is about 0.32(0.28)% at a mass of about 140 GeV for the scenario $\mathcal{A}(\mathcal{B})$, and the limits deteriorate at both ends of the mass range. The results represent first limits on the branching fraction of such a decay channel from direct searches at the LHC. Furthermore, we emphasize that in deriving the limits we have only used a single kinematic distribution in $m_{bb}^{\Delta \text{min}}$. We expect enhanced sensitivity to the charged Higgs boson in future experimental analyses once multivariate discrimination methods are used.

III. MODEL CONSTRAINTS

We can translate the above limits into constraints on the parameter space of the relevant 2HDMs. We take type-I 2HDMs as examples which are less constrained by direct searches at the LHC [16]. One important feature of type-I models is that couplings of the charged Higgs boson and the CP -odd neutral Higgs boson to fermions are both proportional to masses of the fermions divided by $\tan\beta$. The latter is the ratio of vacuum expectation values of the two Higgs doublets. The total branching ratio of the three-body decay can be written as

$$\begin{aligned} B_{H^+}^{\text{sig}}(\mathcal{A}) &= \text{Br}(t \rightarrow H^+ b) \times \text{Br}(H^+ \rightarrow t^{(*)} \bar{b}), \\ B_{H^+}^{\text{sig}}(\mathcal{B}) &= \text{Br}(t \rightarrow H^+ b) \times \text{Br}(H^+ \rightarrow W^+ A) \\ &\quad \times \text{Br}(A \rightarrow b \bar{b}), \end{aligned} \quad (4)$$

for scenario \mathcal{A} and \mathcal{B} , respectively.

In 2HDMs of type-I, the branching ratio $\text{Br}(t \rightarrow H^+ b)$ only depends on M_{H^+} and $\tan\beta$. For that we calculate the partial widths of the top quark at NNLO in QCD for both its SM decay [43] and the decay into the charged Higgs boson [44]. For decays of the charged Higgs boson there are competing channels including $\tau^+ \nu_\tau$, $c \bar{s}$, $t^{(*)} \bar{b}$, and $W^+ A$, while others are negligible in 2HDMs of type-I. The relative weights of fermionic channels only depend on the mass of the charged Higgs boson, where $\tau^+ \nu_\tau$ ($t^{(*)} \bar{b}$) is dominant at small (large) M_{H^+} . For simplicity, we assume the CP -odd Higgs boson A is heavier than the charged Higgs boson in models associated with scenario \mathcal{A} to avoid the decay into $W^+ A$. In models related to scenario \mathcal{B} where

$M_{H^+} - M_A$ is fixed to 85 GeV, the branching fraction to $W^+ A$ is almost 100% for the parameter space of interests, namely, with $\tan\beta \gtrsim 1$. Decays of the Higgs boson A to fermions are dominant. The branching fraction is 82 (0.024)% to a pair of bottom quarks (muons) and is almost independent of $\tan\beta$ and M_{H^+} for the parameter space considered. From above we conclude both $B_{H^+}^{\text{sig}}$ depend only on M_{H^+} and $\tan\beta$ for which we will set constraints on. We calculate the branching fractions of decays of H^+ and A in type-I models using the 2HDMC-1.8.0 program [45].

We reproduce constraints on the parameter space imposed by previous direct searches of a light charged Higgs boson at the LHC for comparisons, all at 13 TeV with an integrated luminosity of about 36 fb^{-1} . They include searches for the $\tau^+ \nu_\tau$ decay channel from both CMS [46] and ATLAS [47]. In addition, there exists a search for the $W^+ A(\mu^+ \mu^-)$ decay channel from CMS [31] assuming $M_{H^+} - M_A = 85 \text{ GeV}$. Based on the 95% CLs limits on the signal strength reported in those analyses, we identify excluded regions of the parameter space as shown in Fig. 3, for the two classes of type-I models considered. The constraints are strongest for models with scenario \mathcal{A} from searches of the $\tau^+ \nu_\tau$ channel. The parameter space is less constrained in models with scenario \mathcal{B} by the CMS search of $W^+ \mu^+ \mu^-$. The results agree with those shown in Ref. [16] except for constraints imposed by the ATLAS search of $\tau^+ \nu_\tau$ that are not considered therein. There also exists a recent analysis from CMS on the $W^+ \mu^+ \mu^-$ channel

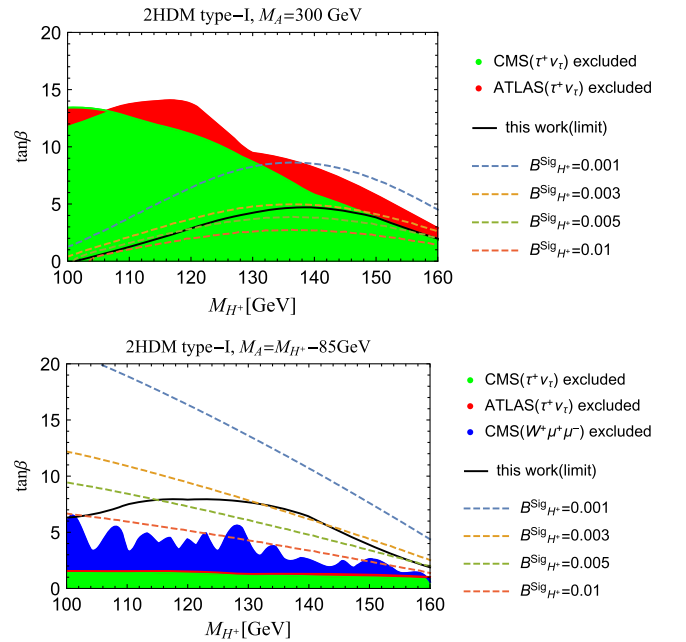


FIG. 3. Excluded regions of the parameter space by various direct searches of the charged Higgs boson at the LHC for the two classes of type-I models considered. Dashed lines represent contours of the respective signal strength ranging from 0.1% to 1%. Regions under the solid curves are excluded by this work.

using a larger data sample of 139 fb^{-1} [48]. They report improved limits on the signal strength by up to a factor of 2 comparing with those in [31].

For the decay channel of $W^+ b \bar{b}$ considered in this work, we plot contours of $B_{H^+}^{\text{sig}}$ in the plane of $\tan\beta$ and M_{H^+} in Fig. 3 for the two classes of type-I models. In models with scenario \mathcal{A} the signal strength can reach at most 0.3% for the allowed parameter space by previous direct searches, with a mass of the charged Higgs boson between 100 and 160 GeV. The new constraints are represented by the solid line which are comparable to the CMS ones for a mass greater than 150 GeV but weaker than the ATLAS constraints. For the class of models with scenario \mathcal{B} , with constraints from previous searches, the signal strength can still be larger than 1%. From the last section the limit on the signal strength is 0.28(0.64)% at M_{H^+} of 140(110) GeV. That excludes the parameter space of $\tan\beta < 5 \sim 8$ for a mass up to 145 GeV, representing the strongest constraints from direct searches. Lastly, we mention that various theoretical and indirect constraints are generally weaker than those from LHC direct searches for type-I models as discussed in Refs. [17–19,49]. For instance, measurements on electroweak precision observables indicate that either of the mass splits between the charged Higgs boson and the two additional neutral Higgs bosons should be small [17]. It is possible that the CP -even Higgs boson is lighter than the charged Higgs boson and contributes via cascade decays similar as the CP -odd Higgs boson. A scan on the full

parameter space of type-I 2HDMs combining all relevant decay channels is desirable which we leave for future investigation.

IV. SUMMARY

We have studied the signature of a light charged Higgs boson produced from top quark pairs at the LHC via its three-body decays into a W boson and a pair of bottom quarks. We obtain the first direct limit on signal strength of the decay channel using the ATLAS measurement at 13 TeV on the relevant final states. The 95% CLs limits the range from 0.28% to 0.74% on $\text{Br}(t \rightarrow H^+ b) \times \text{Br}(H^+ \rightarrow W^+ b \bar{b})$ for a charged Higgs boson with mass between 110 and 160 GeV. The limits are translated into constraints on the parameter space of 2HDMs of type I. We find the strongest constraints on a class of type-I models with a light CP -odd Higgs boson, compared with previous direct searches via other decay channels at the LHC. We encourage dedicated searches by experimental collaborations for further improvements.

ACKNOWLEDGMENTS

The work of J. G. is supported by the National Natural Science Foundation of China under Grants No. 11875189 and No. 11835005. The authors would like to thank Hong-Jian He for useful discussions. We thank the sponsorship from Yangyang Development Fund.

-
- [1] S. Chatrchyan *et al.* (CMS Collaboration), *Phys. Lett. B* **716**, 30 (2012).
 - [2] G. Aad *et al.* (ATLAS Collaboration), *Phys. Lett. B* **716**, 1 (2012).
 - [3] T. D. Lee, *Phys. Rev. D* **8**, 1226 (1973).
 - [4] G. C. Branco, P. M. Ferreira, L. Lavoura, M. N. Rebelo, M. Sher, and J. P. Silva, *Phys. Rep.* **516**, 1 (2012).
 - [5] G. Abbiendi *et al.* (ALEPH, DELPHI, L3, OPAL, LEP Collaborations), *Eur. Phys. J. C* **73**, 2463 (2013).
 - [6] K. Freese, J. T. Liu, and D. Spolyar, *Phys. Lett. B* **634**, 119 (2006).
 - [7] T. Aaltonen *et al.* (CDF Collaboration), *Phys. Rev. Lett.* **107**, 031801 (2011).
 - [8] G. Aad *et al.* (ATLAS Collaboration), *J. High Energy Phys.* **06** (2021) 145.
 - [9] A. M. Sirunyan *et al.* (CMS Collaboration), *J. High Energy Phys.* **07** (2020) 126.
 - [10] A. Arhrib, R. Benbrik, H. Harouiz, S. Moretti, and A. Rouchad, *Front. Phys.* **8**, 39 (2020).
 - [11] D. K. Ghosh, W.-S. Hou, and T. Modak, *Phys. Rev. Lett.* **125**, 221801 (2020).
 - [12] O. Eberhardt, A. P. n. Martínez, and A. Pich, *J. High Energy Phys.* **05** (2021) 005.
 - [13] A. G. Akeroyd, S. Moretti, and M. Song, *J. Phys. G* **49**, 085004 (2022).
 - [14] A. G. Akeroyd, *Nucl. Phys.* **B544**, 557 (1999).
 - [15] A. Arhrib, R. Benbrik, and S. Moretti, *Eur. Phys. J. C* **77**, 621 (2017).
 - [16] P. Sanyal, *Eur. Phys. J. C* **79**, 913 (2019).
 - [17] H. Bahl, T. Stefaniak, and J. Wittbrodt, *J. High Energy Phys.* **06** (2021) 183.
 - [18] A. Arhrib, R. Benbrik, M. Krab, B. Manaut, S. Moretti, Y. Wang, and Q.-S. Yan, *J. High Energy Phys.* **10** (2021) 073.
 - [19] K. Cheung, A. Jueid, J. Kim, S. Lee, C.-T. Lu, and J. Song, *Phys. Rev. D* **105**, 095044 (2022).
 - [20] S. Slabospitskii, [arXiv:2206.02439](https://arxiv.org/abs/2206.02439).
 - [21] M. Aaboud *et al.* (ATLAS Collaboration), *J. High Energy Phys.* **04** (2019) 046.
 - [22] A. Buckley, J. Butterworth, D. Grellscheid, H. Hoeth, L. Lonnblad, J. Monk, H. Schulz, and F. Siegert, *Comput. Phys. Commun.* **184**, 2803 (2013).
 - [23] A. M. Sirunyan *et al.* (CMS Collaboration), *Phys. Lett. B* **803**, 135285 (2020).
 - [24] C. Degrande, R. Frederix, V. Hirschi, M. Ubiali, M. Wiesemann, and M. Zaro, *Phys. Lett. B* **772**, 87 (2017).

- [25] J. Alwall, R. Frederix, S. Frixione, V. Hirschi, F. Maltoni, O. Mattelaer, H. S. Shao, T. Stelzer, P. Torrielli, and M. Zaro, *J. High Energy Phys.* **07** (2014) 079.
- [26] T. Sjöstrand, S. Ask, J.R. Christiansen, R. Corke, N. Desai, P. Ilten, S. Mrenna, S. Prestel, C.O. Rasmussen, and P.Z. Skands, *Comput. Phys. Commun.* **191**, 159 (2015).
- [27] T.-J. Hou *et al.*, *Phys. Rev. D* **103**, 014013 (2021).
- [28] A. Alloul, N.D. Christensen, C. Degrande, C. Duhr, and B. Fuks, *Comput. Phys. Commun.* **185**, 2250 (2014).
- [29] M. Czakon, P. Fiedler, and A. Mitov, *Phys. Rev. Lett.* **110**, 252004 (2013).
- [30] M. Czakon and A. Mitov, *Comput. Phys. Commun.* **185**, 2930 (2014).
- [31] A. M. Sirunyan *et al.* (CMS Collaboration), *Phys. Rev. Lett.* **123**, 131802 (2019).
- [32] T. Gleisberg, S. Hoeche, F. Krauss, M. Schonherr, S. Schumann, F. Siegert, and J. Winter, *J. High Energy Phys.* **02** (2009) 007.
- [33] R. D. Ball *et al.* (NNPDF Collaboration), *J. High Energy Phys.* **04** (2015) 040.
- [34] T. Ježo, J. M. Lindert, N. Moretti, and S. Pozzorini, *Eur. Phys. J. C* **78**, 502 (2018).
- [35] S. Frixione, P. Nason, and G. Ridolfi, *J. High Energy Phys.* **09** (2007) 126.
- [36] M. Aaboud *et al.* (ATLAS Collaboration), Report No. ATLAS-PHYS-PUB-2016-020 (2016).
- [37] M. V. Garzelli, A. Kardos, and Z. Trócsányi, *J. High Energy Phys.* **03** (2015) 083.
- [38] G. Bevilacqua, M. V. Garzelli, and A. Kardos, *arXiv:1709.06915*.
- [39] A. Denner, J.-N. Lang, and M. Pellen, *Phys. Rev. D* **104**, 056018 (2021).
- [40] G. Bevilacqua, H.-Y. Bi, H.B. Hartanto, M. Kraus, M. Lupattelli, and M. Worek, *J. High Energy Phys.* **08** (2021) 008.
- [41] G. Bevilacqua, H.-Y. Bi, H.B. Hartanto, M. Kraus, M. Lupattelli, and M. Worek, *arXiv:2202.11186*.
- [42] A. Read, *J. Phys. G* **28**, 2693 (2002).
- [43] J. Gao, C. S. Li, and H. X. Zhu, *Phys. Rev. Lett.* **110**, 042001 (2013).
- [44] X.-M. Shen, Y. Hu, C. Sun, and J. Gao, *J. High Energy Phys.* **05** (2022) 157.
- [45] D. Eriksson, J. Rathsman, and O. Stal, *Comput. Phys. Commun.* **181**, 189 (2010).
- [46] A. M. Sirunyan *et al.* (CMS Collaboration), *J. High Energy Phys.* **07** (2019) 142.
- [47] M. Aaboud *et al.* (ATLAS Collaboration), *J. High Energy Phys.* **09** (2018) 139.
- [48] G. Aad *et al.* (ATLAS Collaboration), Report No. ATLAS-CONF-2021-047, 2021.
- [49] J. Ren, R.-Q. Xiao, M. Zhou, Y. Fang, H.-J. He, and W. Yao, *J. High Energy Phys.* **06** (2018) 090.